



# AC conductivity and dielectric behavior of poly (o-phenylenediamine)/TiO<sub>2</sub> nanocomposites

Archana S \*

Department of Chemistry, SMK Fomra Institute of Technology, Chennai, Tamil Nadu, INDIA

\*Corresponding author E-mail:

## Abstract

Poly (o-phenylenediamine) and their nanocomposites with TiO<sub>2</sub> nanoparticles were synthesized using oxidative polymerization technique and the polymer nanocomposites were characterized using spectral techniques like FT-IR, UV-VIS spectroscopy and the morphology have been analyzed by XRD, SEM and TEM. The stability of the prepared polymer nanocomposites was studied using TGA, DTA and found to have high thermal stability. The study of ac conductivity, dielectric property revealed that the formed nanocomposites are semiconducting in nature and can be widely used in the field of energy storage and semiconductor devices, in diodes, batteries etc.

**Keywords:** Polyphenylenediamine; Nanocomposites; Dielectric Property; Ac Conductivity.

## 1. Introduction

Polyphenylenediamines are considered to be conductive polymers which have attracted attention lately because they display high gas separation ability (Mohaseen et al. 2012 & Pandi Boomi et al. 2014) and lyotropic liquid crystallinity (Pandi Boomi et al. 2013 & Pandi Boomi et al. 2014) Furthermore, it is reported that polyphenylenediamines produced by chemically oxidative polymerization with sodium, potassium, or ammonium persulfate as oxidants show ladder and ladder-like structures having highly aromatic nitrogenous heterocycles and show unusually high thermostability (Pandi Boomi et al. 2013 & Mansour Ghaffari-Moghaddam et al. 2014 & Yong Kong et al. 2013 & Mahasweta Nandi et al. 2011 & Mei-Rong Huang et al. 2001 & Garjonyte et al. 1999 & Zhang et al 2011). The nitrogenous heterocyclic ladder structure is considered to be of great benefit to the preparation of advanced air separation membranes (Anderson et al. 1991. Moreover, the solubility of the polyphenylenediamines in most of the common organic solvents is low and depends on solvent composition and on the oxidant that was used for polymerization (Myler et al. 1997 & Liu et al. 2008). Only a few studies on oxidative homopolymerization of three phenylenediamine isomers have been described (Cao et al. 1993 & cataldo. 1996).

Various methods are available for the synthesis of polyphenylenediamines. However, the most widely used techniques are electrochemical and chemical oxidative polymerization methods. The chemical method is important to produce polyphenylenediamines on large scale. Several oxidizing agents have been used in the polymerization of polyphenylenediamines. Poly (o-phenylenediamine) (PoPDA) hollow spheres using ammonium persulfate (APS) and PoPDA nanofibres using chlorauric acid. Isomers of polyphenylenediamine were prepared using APS as an oxidant and their copolymer with polyaniline have been reported. Poly (p-phenylenediamine) (PpPDA) was chemically prepared using potassium persulfate and their voltammetric studies and the

electrochromic behavior had been analyzed (premasiri et al. 1995 & Chan et al. 1991).

A rapid, templateless, surfactantless approach was used to prepare microfibrils by simply mixing of aqueous cupric sulfate and o-phenylenediamine (oPD) solutions at room temperature (Li et al. 2001). Microfibers of PoPDA have been prepared by direct mixing of aqueous solution of ferric chloride and oPD solution at room temperature (Sestrem et al. 2009). PoPDA hollow multi-angular microrods have been synthesized at 10°C by an interfacial process using ferric chloride and oPD and the possible formation mechanism of the structure has been proposed (Sestrem et al. 2010). Microrods of poly (o-phenylenediamine) were synthesized by a templateless method using ferric chloride as an oxidant (Huang et al. 2001).

In the present study, PoPDA and their nanocomposites with TiO<sub>2</sub> nanoparticles were synthesized using FeCl<sub>3</sub> as an oxidant and studied applications like dielectric property and ac conductivity.

## 2. Materials and methods

### 2.1. Materials

The monomer o-phenylenediamine, ferric chloride, surfactant Sodium Dodecyl Sulfate was purchased from Merck, all the other chemicals and reagents were of Analytical Grade and used as received without further purification. The nanoparticles of TiO<sub>2</sub> were purchased from Sigma Aldrich of particle size 60-70nm.

### 2.2. Methods synthesis of poly (o-phenylenediamine) with TiO<sub>2</sub> nanoparticles

The equimolar volume of o-phenylenediamine and hydrochloric acid was prepared and TiO<sub>2</sub> is added in the weight percentages of 10, 20 and 30% to the above solution and kept for vigorous stirring to keep the TiO<sub>2</sub> suspended in the solution. To this, SDS was

added as an emulsifier and ferric chloride was added drop wise as an oxidant. The obtained solutions were kept for stirring at room temperature for 6 hours to polymerize the monomers. The poly (o-phenylenediamine)-TiO<sub>2</sub> nanocomposites (PoPDA/TiO<sub>2</sub>) precipitate was collected on filtration, washed with deionised water followed by methanol to remove the oligomers and unreacted monomers present in the polymers (Aashish Roy et al. 2013).

### 2.3. Characterization technique

The FT-IR spectrum of the synthesized samples was recorded on an ABB-MB-3000 FT-IR spectrometer in KBr medium. The UV-Vis spectrum of polymers was taken using Perkin Elmer Lambda UV-Vis- Spectrometer by dissolving the polymers in DMSO as a solvent. The XRD was measured with Bruker AXS D8 Advance using Cu as X-ray source at the Wavelength of 1.5406 Å of angular range from 3° to 135°. Scanning electron microscopy was used to study the morphology of the synthesized polymers using JEOL, JSM-6390LV model. High-resolution transmission electron microscopy was measured using Tecnai T20 G2 S-TWIN of operating voltage 250 kV. TG/DTA was recorded using Perkin Elmer STA 6000 model. The Broadband Dielectric Spectrometer (BDS) was measured in pellet form using NOVOCONTROL Technologies, GmbH & Co. Germany, Concept 80 model. Differential Scanning Calorimetry (DSC) was measured using Mettler Toledo DSC 822e from room temperature to 300°C.

## 3. Results and discussion

### 3.1. FT-IR spectra of poly (o-phenylenediamine) with different concentrations of TiO<sub>2</sub> nanoparticles

The FT-IR spectrum of PoPDA with 10, 20 and 30% titanium dioxide which is represented as PoPDA/10%TiO<sub>2</sub>, PoPDA/20%TiO<sub>2</sub> and PoPDA/30%TiO<sub>2</sub> shows a single band at 3352 cm<sup>-1</sup> is due to the N-H stretching vibrations of the -NH-group. The two peaks at 3413, 3195 cm<sup>-1</sup> are ascribed to the asymmetrical and symmetrical of N-H stretching vibrations of NH<sub>2</sub> group. Two strong peaks at 1688 cm<sup>-1</sup> and 1520 cm<sup>-1</sup> are associated with the stretching vibrations of C=N and C=C group in phenazine ring. The peaks at 1374 cm<sup>-1</sup> and 1244 cm<sup>-1</sup> are associated with C-N-C stretching in the benzenoid and quinoid imine units. Furthermore, the bands at 752 cm<sup>-1</sup> and 582 cm<sup>-1</sup> are characteristic of C-H out-of-plane bending vibrations of benzene nuclei in the phenazine skeleton (Fig. 1). When compared to the polymer, the wave numbers of polymer nanocomposites have slightly shifted to longer wave number due to formation of hydrogen bonding between oxygen of TiO<sub>2</sub> and hydrogen of -NH- group present in the polymer (Mona et al. 2011). In addition to the above peaks, the presence of peak at 486 cm<sup>-1</sup> which is due to M-O bond stretching vibration of TiO<sub>2</sub> metal oxides confirms the incorporation of TiO<sub>2</sub> into the polymeric matrix and the incorporation of SDS into the polymeric backbone is confirmed from the peak at 1049cm<sup>-1</sup> which is due to S=O stretching vibration.

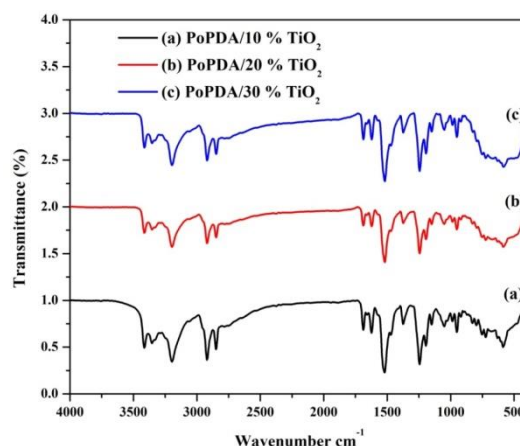


Fig. 1: FT-IR Spectra of Poly (o-Phenylenediamine) with Different Concentrations of TiO<sub>2</sub> Nanoparticles.

### 3.2. UV-VIS spectra of poly (o-phenylenediamine) with different concentrations of TiO<sub>2</sub> nanoparticles

The UV-Vis spectra of PoPDA with 10%, 20% and 30% TiO<sub>2</sub> show major peaks at about 282 and 441 nm. The band near 441 nm is assigned to  $\pi-\pi^*$  transition associated with the phenazine ring conjugated to the two lone pairs of electrons present on the nitrogen of the NH<sub>2</sub> groups, the peak is broad and it suggests the existence of quinoneimine moieties. The other peak at about 282 nm is mainly assigned to the  $\pi-\pi^*$  transitions of the benzenoid and quinoid structures. The UV-Vis spectra of PoPDA synthesized at different concentrations of TiO<sub>2</sub> nanoparticles are given in Fig. 2.

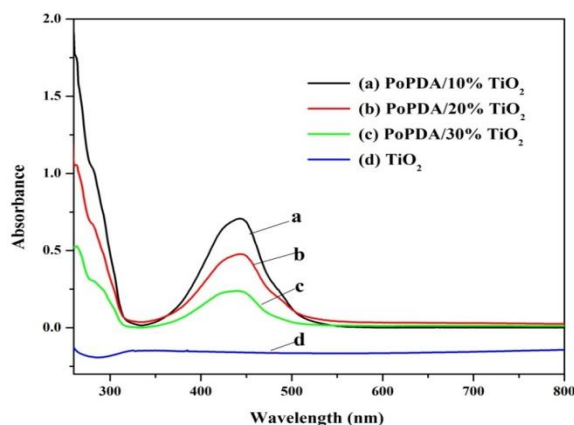
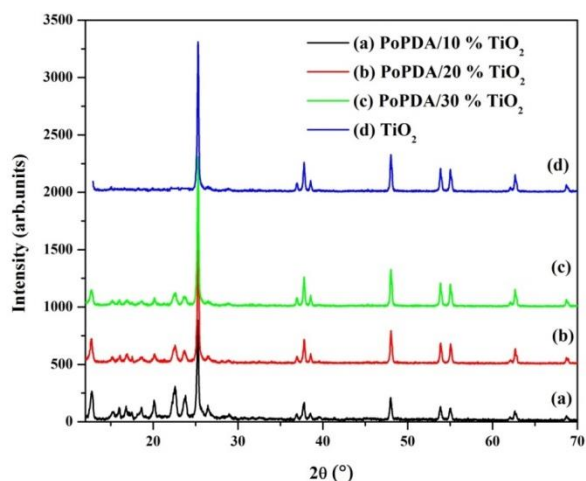


Fig. 2: UV-Vis Spectra of Poly (o-Phenylenediamine) with Different Concentrations of TiO<sub>2</sub> Nanoparticles.

### 3.3. XRD of poly (o-phenylenediamine) nanocomposites with different concentrations of TiO<sub>2</sub> nanoparticles

The XRD spectra of PoPDA nanocomposites with the different concentrations of TiO<sub>2</sub> like 10, 20, 30 wt % are given in the Fig. 3. From the spectra it is observed, the peaks at  $2\theta = 25.38, 37.88, 48.08, 53.98,$  and  $55.18$  can be assigned to the diffractions of the (1 0 1), (0 0 4), (2 0 0), (1 0 5), and (2 1 1) crystal planes of anatase phase of TiO<sub>2</sub>. The characteristic diffraction peaks observed at 27.48 and 36.18 can be attributed to the (1 1 0) and (1 0 1) faces of rutile phase in TiO<sub>2</sub> (Meirong Wang et al. 2013).

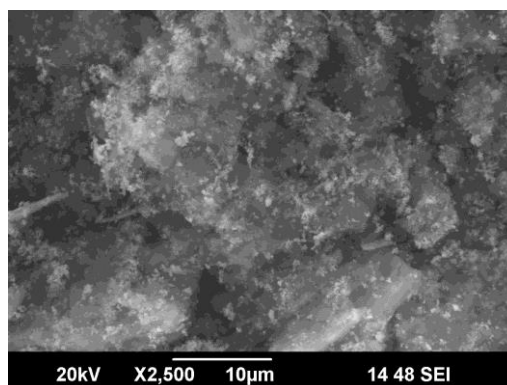
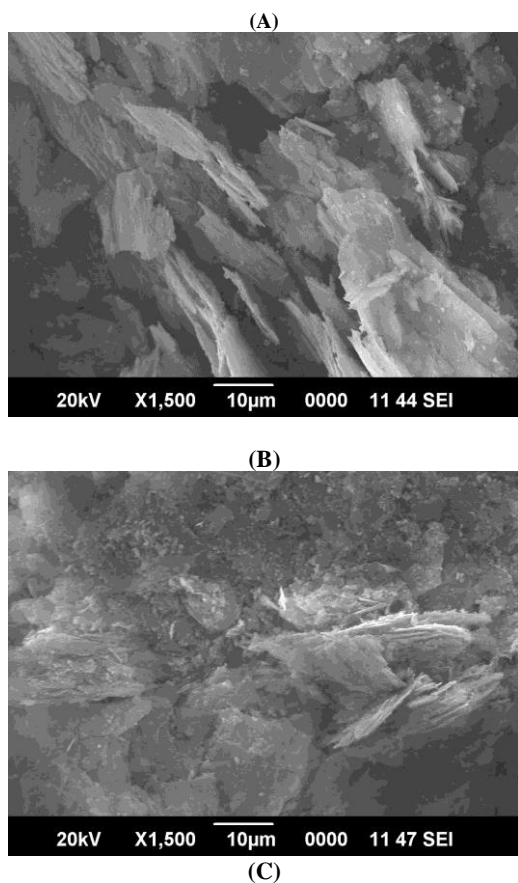
The XRD patterns of PoPDA nanocomposites show the characteristic peaks not only for the PoPDA which is  $5^\circ < 2\theta < 35^\circ$  but also for the TiO<sub>2</sub> nanoparticles, proving the existence of TiO<sub>2</sub> nanoparticles within the polymer nanocomposite. This confirms that the PoPDA nanocomposites become more crystalline as the concentration of TiO<sub>2</sub> is increased. The PoPDA has not affected the crystallization behavior of TiO<sub>2</sub> nanoparticles (Pandi Muthirulan et al. 2013) in the nanocomposite formed as it is evident from the Fig. 3.



**Fig. 3:** XRD Spectra of Poly (o-Phenylenediamine) with Different Concentrations of  $\text{TiO}_2$  Nanoparticles.

### 3.4. SEM images of poly (o-phenylenediamine) nanocomposites with different concentrations of $\text{TiO}_2$ nanoparticles

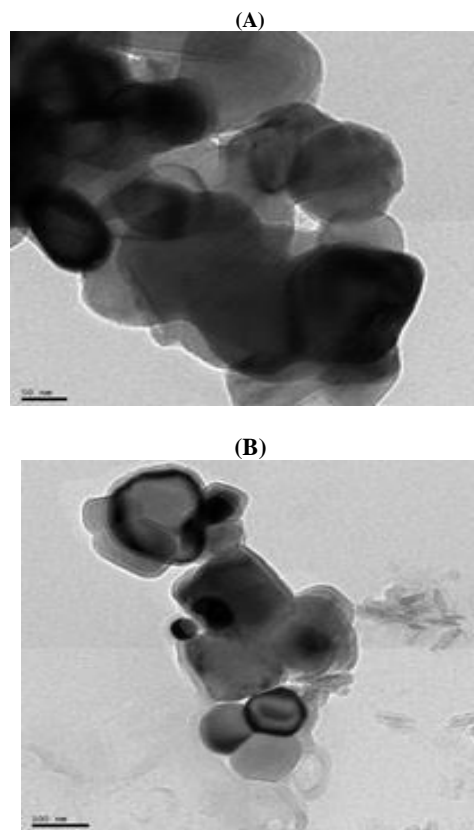
The polymer nanocomposites with different concentration of  $\text{TiO}_2$  nanoparticles are found to have agglomerated granular in shape and has crystalline in nature. As the concentration of  $\text{TiO}_2$  nanoparticles increased the aggregation of nanoparticles on the polymers was found to increase and it uniformly distributed throughout the nanocomposite. The  $\text{TiO}_2$  nanocomposites having spherical in shape have been aggregated on the surface of the PoPDA nanocomposites and thus the PoPDA with 30% $\text{TiO}_2$  gives the properties of both PoPDA and  $\text{TiO}_2$  which is evident from XRD patterns of highly crystalline nature of polymer nanocomposites (Fig. 4 a-c).



**Fig. 4:** (A-C) SEM Images of PoPDA with 10, 20 and 30%  $\text{TiO}_2$  Nanoparticles.

### 3.5. TEM study of poly (o-phenylenediamine) with 30% $\text{TiO}_2$ nanoparticles

The particle size of the PoPDA with 30%  $\text{TiO}_2$  nanoparticles was imaged using HRTEM and found to have aggregated core shell type of morphology with the spherical like particles. The particle size of the synthesized polymer nanocomposites falls in the range of 60-70 nm as it is evident from the Fig. 5 with different magnifications. The entire surface of the  $\text{TiO}_2$  nanoparticles were surrounded by uniform thin layer of PoPDA and the  $\text{TiO}_2$  nanoparticles are well dispersed in the polymeric matrix. Moreover, the outer shell of the  $\text{TiO}_2$  nanoparticles exhibited a fine increment in brightness due to the presence of polymer compared with the dark inner core, which confirmed the formation of core-shell feature of the PoPDA nanocomposites with 30% of  $\text{TiO}_2$  nanoparticles. The formation of PoPDA encapsulated  $\text{TiO}_2$  core-shell nanocomposites were attributed to the strong electrostatic interaction between PoPDA and  $\text{TiO}_2$  nanoparticles (Meirong Wang et al. 2013).



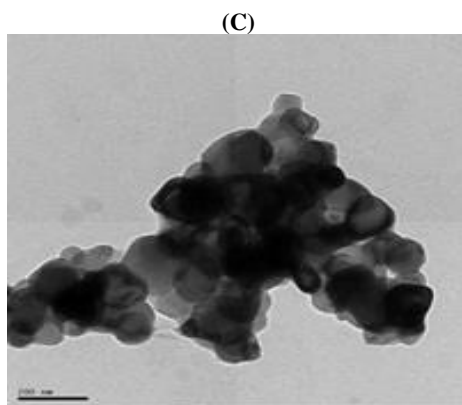


Fig. 5: (A-C) HRTEM Images of PoPDA/ 30% TiO<sub>2</sub> Nanocomposites at Different Magnification.

### 3.6. TGA and DTA of poly (o-phenylenediamine) nanocomposites with different concentrations of TiO<sub>2</sub> nanoparticles

The three stages of thermal transition that lead to weight loss PoPDA with different concentrations of TiO<sub>2</sub> like 10%, 20% and 30% are exhibited in Fig. 6. The first thermal transition from 200 to 210 °C is ascribed to the removal of dopant molecules. The loss of low molecular weight oligomers or side products present in the polymeric compound are due to the second thermal transition from 230 to 290°C. The third transition is observed between 300 °C to 732 °C with a weight loss of ~30%, and this can be attributed to the degradation of benzenoid and quinonoid repeating units present in the polymeric backbone. The residue present at the end of the heating process is 0.99 mg for PoPDA with 10%TiO<sub>2</sub>, 1.6625mg for PoPDA with 20%TiO<sub>2</sub> and 4.081mg for PoPDA with 30%TiO<sub>2</sub>.The amount of residue is more when the percentage of TiO<sub>2</sub> increased which also confirms the incorporation of metal oxide into the polymer. The DTA curves of PoPDA with 10%, 20% and 30% TiO<sub>2</sub> nanoparticles (Fig. 7.) displayed exothermic peak at 400–705 °C. This may be due to pyrolysis of the organic group, dehydroxylation and collapse of the layered structure, and recrystallization of the pyrolysis product into oxides (Ukrainczyk et al. 1997).

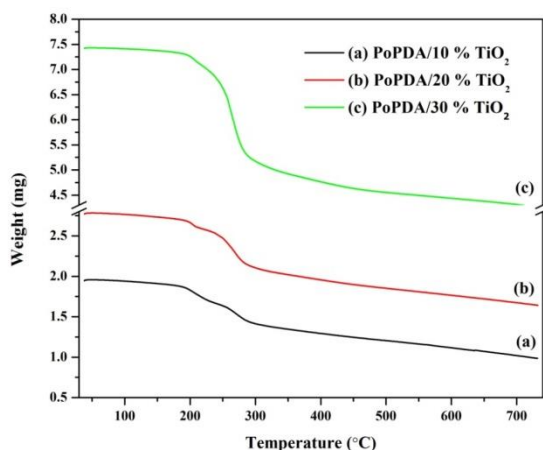


Fig. 6: TGA Spectra of Poly (o-Phenylenediamine) Nanocomposites with Different Concentrations of TiO<sub>2</sub> Nanoparticles.

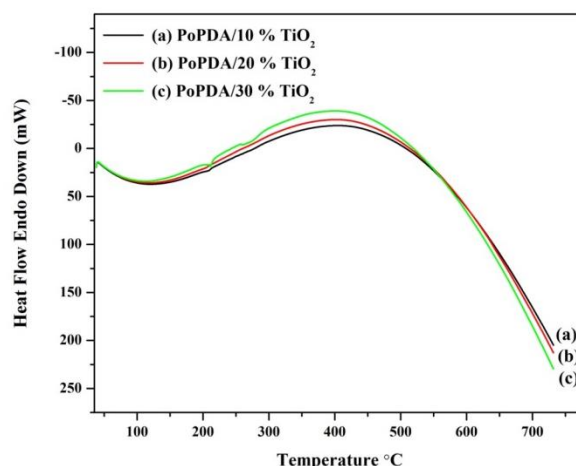


Fig. 7: DTA Spectra of Poly (o-Phenylenediamine) Nanocomposites with Different Concentrations of TiO<sub>2</sub> Nanoparticles.

### 3.7. DSC spectrum of poly (o-phenylenediamine) nanocomposites with TiO<sub>2</sub> nanoparticles

The DSC spectrum of poly (o-phenylenediamine) with 30 weight percentage of TiO<sub>2</sub> nanoparticles shows an endothermic peak at 213°C is due to the glass transition temperature (Fig. 8.). The polymer starts to melt above 260°C which is shown by endothermic peak at 270.22°C which is characteristics of melting temperature.

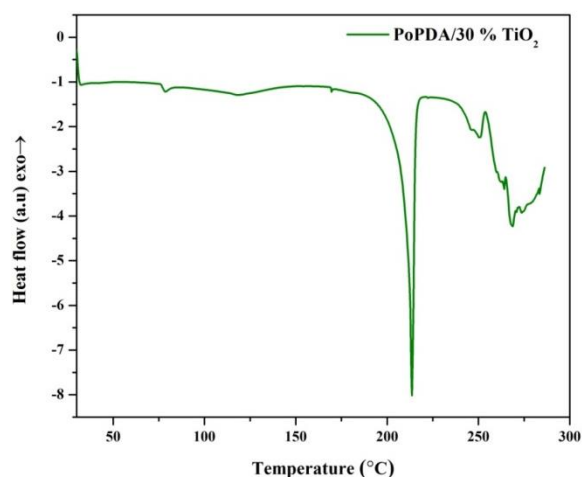


Fig. 8: DSC Spectrum of Poly (o-Phenylenediamine) Nanocomposites with TiO<sub>2</sub> Nanoparticles.

### 3.8. Study of AC conductivity

The complex impedance spectra of synthesized polymers and the polymer nanocomposites with different weight percentages of TiO<sub>2</sub> nanoparticles were evaluated by plotting real ( $Z'$ ) and imaginary part ( $Z''$ ) of complex impedance. From the plot the bulk resistance ( $R_b$ ) for the prepared samples was evaluated by analyzing the impedance data using ZSimpdemo software. The conductivity values of polymers and their nanocomposites with 10, 20 and 30% of TiO<sub>2</sub> nanoparticles were evaluated using bulk resistance ( $R_b$ ) using the formula,

$$\sigma = (t / A) (1 / R_b) S/cm$$

Where,  $t$  is the thickness of the pellet,  $A$  is the area of pellet and  $R_b$  is the bulk resistance of the pellet.

The conductivity of the PoPDA nanocomposites increases with the addition of TiO<sub>2</sub> nanoparticles from the order of  $10^{-7}$  to the order of  $10^{-5}$  and this may be due to the incorporation of TiO<sub>2</sub>

nanoparticles in to the polymeric matrix. The conductivity of the polymer nanocomposites synthesized with 10, 20, 30 %  $\text{TiO}_2$  nanoparticles (Fig. 9) are found to be  $1.2753 \times 10^{-5}$  S/cm,  $2.2590 \times 10^{-5}$  S/cm and  $2.4417 \times 10^{-5}$  S/cm respectively. There was a slight increase in the conductivity with increase in the concentration of  $\text{TiO}_2$ .

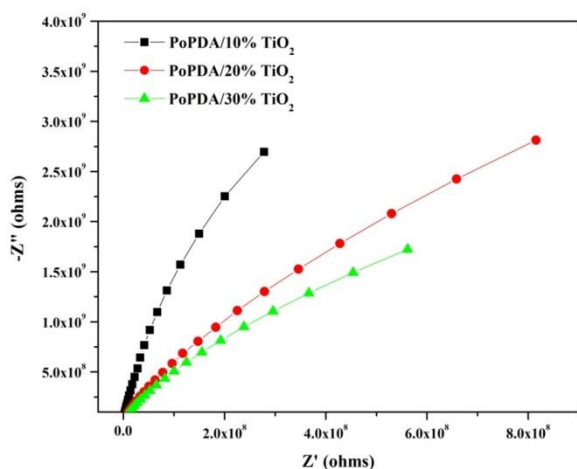


Fig. 9: Complex Impedance Spectra of Poly (o-Phenylenediamine) and their Nanocomposites with Different Concentrations of  $\text{TiO}_2$  Nanoparticles

### 3.9. Variation of ac conductivity with frequency

The  $\sigma_{ac}$  conductivity of PoPDA nanocomposites with 10%, 20% and 30%  $\text{TiO}_2$  nanoparticles were found to increase linearly with increasing frequency from 10Hz to 1 MHz for all the prepared polymer nanocomposites. The PoPDA with  $\text{TiO}_2$  nanocomposites are found to have higher conductivity than the PoPDA with and without SDS (Fig. 10). The variation of ac conductivity of nanocomposites obeyed by "Universal law" which was used to describe conductive behavior of disordered materials (Ke et al. 2009 & Li Yu et al. 2012).

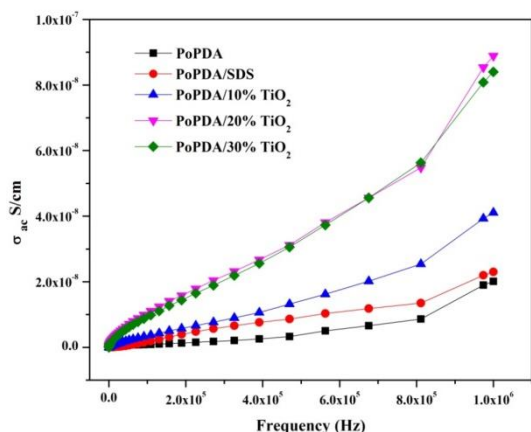


Fig. 10: Plot of  $\sigma_{ac}$  Vs Frequency of Poly (o-Phenylenediamine) and their Nanocomposites with Different Concentrations of  $\text{TiO}_2$  Nanoparticles.

### 3.10. Dielectric analysis

#### 3.10.1. Dielectric analysis of poly (o-phenylenediamine) nanocomposites with different concentrations of $\text{TiO}_2$ nanoparticles

The plot of real and imaginary part of complex permittivity against frequency for PoPDA, PoPDA synthesized with SDS and the polymer nanocomposites prepared with different concentrations of  $\text{TiO}_2$  nanoparticles shows the characteristics of charged carrier systems (Fig. 11 and 12). In all the polymers and their nanocomposites, both  $\epsilon'$  and  $\epsilon''$  increase with the decrease in frequency. Generally at any particular frequency, the dielectric per-

mittivity is found to increase and this behavior is more pronounced at lower frequencies having the value of 1.35 for PoPDA synthesized with 30%  $\text{TiO}_2$  (below 2 Hz). The increment in permittivity with decrease of frequency reveals that the systems exhibit strong interfacial polarization at low frequency. As reported by the other authors (Lee et al. 1993 & Muhammad et al. 2005) the strong low frequency dispersion for  $\epsilon'$  and no loss peak for  $\epsilon''$  are characteristics of charged carrier systems (Bluma et al. 2006).

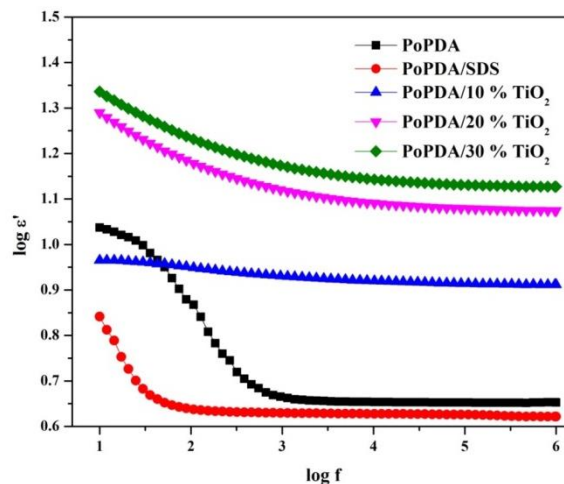


Fig. 11: Plot of  $\log \epsilon'$  Vs  $\log$  Frequency of Poly (o-Phenylenediamine) and their Nanocomposites with Different Concentrations of  $\text{TiO}_2$  Nanoparticles.

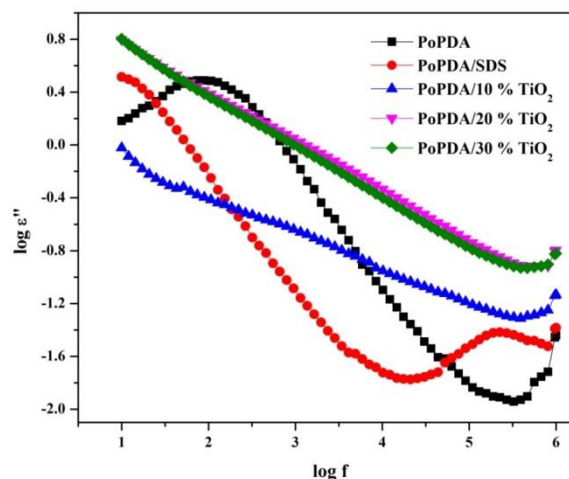
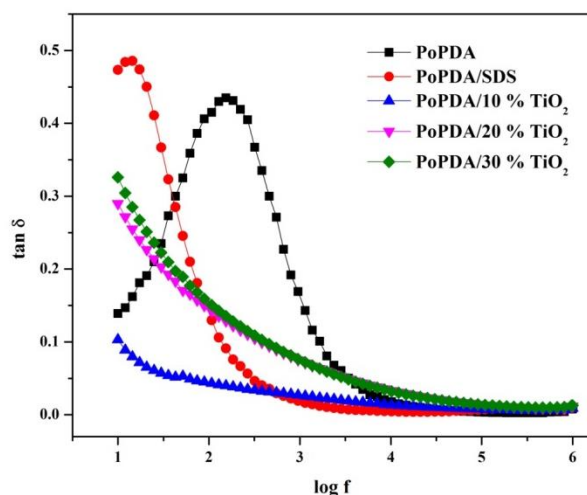


Fig. 12: Plot of  $\log \epsilon''$  Vs  $\log$  Frequency of Poly (o-Phenylenediamine) and their Nanocomposites with Different Concentrations of  $\text{TiO}_2$  Nanoparticles.

#### 3.10.2. Variation of tangent loss with frequency

The PoPDA nanocomposites prepared with 10%, 20% and 30%  $\text{TiO}_2$  nanoparticles, the  $\tan \delta$  against frequency was plotted (Fig. 13). The broad loss peak appeared in PoPDA is completely eliminated for the polymer nanocomposites and this is due to the inorganic nanoparticles which appear to reduce the chain movement of the polymer through physical bonding or through confinement (Roy et al. 2005).



**Fig. 13:** Plot of  $\tan \delta$  Vs log Frequency of Poly (o-Phenylenediamine) and their Nanocomposites with Different Concentrations of  $\text{TiO}_2$  Nanoparticles.

#### 4. Conclusion

The  $\text{TiO}_2$  nanocomposites of PoPDA have been successively prepared via chemical oxidative polymerization method. The synthesized polymer nanocomposites were characterized using FT-IR, UV-Vis spectroscopy and from the result it is confirmed the formation of the polymers. The morphology was studied by XRD, SEM, TEM and confirmed that the synthesized nanocomposites were of highly crystalline in nature and the formation of core shell type morphology of  $\text{TiO}_2$  nanoparticles incorporated into the polymer shell were confirmed. From the thermal analysis like TG/DTA, DSC, the polymer stability were analyzed and found to be thermally more stable. The PoPDA/ $\text{TiO}_2$  nanocomposites have increased in electrical conductivity when compare to the PoPDA. Dielectric analysis of the polymer and their nanocomposites shows that these materials can be used as energy storage devices, semiconductor devices, piezoelectric transducers, dielectric amplifiers etc.

#### References

- [1] Mohaseen, S., Tamboli, Milind, V., Kulkarni, Rajendra, H., Patil, Wasudev, N. Gade., Shalaka, C. Navale., Bharat B. Kale, 2012. Colloids and Surfaces B: Biointerfaces, 92, 35– 41. <https://doi.org/10.1016/j.colsurfb.2011.11.006>.
- [2] Pandi Boomi, Halliah Gurumallesh Prabu, Paramasivam Manisamkar and Sundaram Ravikumar, 2014. Applied Surface Science, 300, 66–72. <https://doi.org/10.1016/j.apsusc.2014.02.003>.
- [3] Pandi Boomia, Halliah Gurumallesh Prabua, Jayaraman Mathiyarasu, 2013. Colloids and Surfaces B: Biointerfaces, 103, 9– 14. <https://doi.org/10.1016/j.colsurfb.2012.10.044>.
- [4] Pandi Boomi, Halliah Gurumallesh Prabu, Jayaraman Mathiyarasu, 2014. European Journal of Medicinal Chemistry, 72, 18–25. <https://doi.org/10.1016/j.ejmech.2013.09.049>.
- [5] Pandi Boomi, Halliah Gurumallesh Prabu, 2013. Colloids and Surfaces A: Physicochemical Engineering Aspects, 429, 51– 59. <https://doi.org/10.1016/j.colsurfa.2013.03.053>.
- [6] Mansour Ghaffari-Moghaddam, Hassan Eslahi, 2014. Arabian Journal of Chemistry, 7 (5) 846–855. <https://doi.org/10.1016/j.arabj.2013.11.011>.
- [7] Yong Kong, Wei Li, Zhiliang Wang, Chao Yao, Yongxin Tao, 2013. Electrochemistry Communications, 26, 59–62. <https://doi.org/10.1016/j.elecom.2012.10.016>.
- [8] Mahasweta Nandi, Swapan Kumar Das, Saurav Giri, Asim Bhaumik, 2011. Microporous and Mesoporous Materials, 142, 557–563. <https://doi.org/10.1016/j.micromeso.2010.12.048>.
- [9] Mei-Rong Huang, Xin-Gui Li, Yuliang Yang, 2001. Polymer Degradation and Stability, 71, 31–38. [https://doi.org/10.1016/S0141-3910\(00\)00137-3](https://doi.org/10.1016/S0141-3910(00)00137-3).
- [10] Garjonyte, R., Malinauskas, A., 1999. Sensors and Actuators B, 56, 85–92. [https://doi.org/10.1016/S0925-4005\(99\)00163-X](https://doi.org/10.1016/S0925-4005(99)00163-X).

- [11] Zhang, Y., Li, H., Luo, Y., Shi, X., Tian, J., 2011. Plos one, 6, 1–11. <https://doi.org/10.1371/annotation/4056d03c-20ed-4eca-9568-3e9400e2312e>.
- [12] Anderson, MR., Mattes, BR., Reiss, H., Kaner, RB, 1991. Science, 252, 1412–5. <https://doi.org/10.1126/science.252.5011.1412>.
- [13] Myler, S., Eaton, S., Higson, SP., 1997. Analytica Chimica Acta, 357, 55–61. [https://doi.org/10.1016/S0003-2670\(97\)00558-8](https://doi.org/10.1016/S0003-2670(97)00558-8).
- [14] Liu, Z., Zu, Y., Guo, S., Fu, Y., Zhang, Y., Liang, H., 2008. Material Science Engineering C, 28, 1284–8. <https://doi.org/10.1016/j.msec.2007.12.002>.
- [15] Cao, Y., Smith, P., 1993. Polymer, 34, 3139–43. [https://doi.org/10.1016/0032-3861\(93\)90381-J](https://doi.org/10.1016/0032-3861(93)90381-J).
- [16] Cataldo, F., 1996. European Polymer Journal, 32, 43–50. [https://doi.org/10.1016/0014-3057\(95\)00118-2](https://doi.org/10.1016/0014-3057(95)00118-2).
- [17] Premasiri, AH. Euler, WB. 1995. Macromolecular Chemistry and Physics, 196, 3655–66. <https://doi.org/10.1002/macp.1995.021961118>.
- [18] Chan, HSO, Ng, SC., Hor, TSA. Sun, J., Tan, KL. Tan, BTG. 1991. European Polymer Journal, 27, 1303–8. [https://doi.org/10.1016/0014-3057\(91\)90069-Z](https://doi.org/10.1016/0014-3057(91)90069-Z).
- [19] Li, X-G., Huang, M-R., Chen, R-F., Jin, Y., Yang, Y-L., 2001. Journal of Applied Polymer Science, 81, 3107–31016. <https://doi.org/10.1002/app.1762>.
- [20] Sestrem, RH. Ferreir, DC. Landers, R., Temperini, MLA. Do Nascimento, GM., 2009. Polymer, 50, 6043–8. <https://doi.org/10.1016/j.polymer.2009.10.028>.
- [21] Sestrem, RH. Ferreir, DC. Landers, R., Temperini, MLA. Do Nascimento, GM., 2010. European Polymer Journal, 46, 484–93. <https://doi.org/10.1016/j.eurpolymj.2009.12.007>.
- [22] Huang, M-R., Li, X-G., Yang, Y., 2001. Polymer Degradation and Stability, 71, 31–8. [https://doi.org/10.1016/S0141-3910\(00\)00137-3](https://doi.org/10.1016/S0141-3910(00)00137-3).
- [23] Aashish Roy, Ameena Parveen, Raghunandan Deshpande, Ravishankar Bhat, Anilkumar Koppalkar, 2013. Journal of Nanoparticle Research, 15:1337 <https://doi.org/10.1007/s11051-012-1337-z>.
- [24] Mona H. Abdel Rehim, Nahla Ismail, Abd El-Rahman A.A. Badawy, Gamal Turkey, 2011. Materials Chemistry and Physics, 128, 507–513. <https://doi.org/10.1016/j.matchemphys.2011.03.037>.
- [25] Meirong Wang, Huaihao Zhang, Chengyin Wang, Guoxiu Wang, 2013. Electrochimica Acta, 106, 301–306. <https://doi.org/10.1016/j.electacta.2013.05.097>.
- [26] Pandi Muthirulan, Chenthamarai Kannan Nirmala Devi, Mariappan Meenakshi Sundaram, 2013. Journal of Environmental Chemical Engineering, 1, 620–627. <https://doi.org/10.1016/j.jece.2013.06.025>.
- [27] Ukrainczyk, L., Bellman, RA., Anderson, AB., 1997. Journal of Physics and Chemistry B, 101(4), 531–539. <https://doi.org/10.1021/jp9629371>.
- [28] Ke, SM., Huang. HT. Ren, L., Wang, YJ, 2009. Journal of Applied Physics, 105 (9) 1–3. <https://doi.org/10.1063/1.3125271>.
- [29] Li Yu, Yihe Zhang, Wangshu Tong, Jiwu Shang, Fengzhu Lv, Paul K. Chu, Wenmin Guo, 2012. Composites: Part A, 43, 2039–2045. <https://doi.org/10.1016/j.compositesa.2012.06.001>.
- [30] Lee, HT. Liao, CS., Chen, SA. 1993. Makromol Chem, 194, 2443. <https://doi.org/10.1002/macp.1993.021940903>.
- [31] Muhammad AKRAM, Athar JAVED, Tasneem Zahra RIZVI, 2005. Turkish Journal of Physics, 29, 355–362.
- [32] Bluma G. Soares, Maria Elena Leyva, Guilherme M.O. Barra, Dipak Khastgir, 2006. European Polymer Journal, 42, 676–686. <https://doi.org/10.1016/j.eurpolymj.2005.08.013>.
- [33] Roy M., Nelson J.K., MacCrone R.K., Schadler L.S., 2005. Polymer Nanocomposite Dielectrics -The Role of the Interface.